Rapid Communications

Spins and electromagnetic moments of $^{101-109}$Cd

D. T. Yordanov,[1,2,3,*] D. L. Balabanski,[4] M. L. Bissell,[5,6] K. Blaum,[2] A. Blazhev,[7] I. Budinčević,[6] N. Frömmgen,[8] Ch. Geppert,[9,8,10] H. Grawe,[10] M. Hammen,[8] K. Kreim,[2] R. Neugart,[2,8] G. Neyens,[6,3] and W. Nörtershäuser[9,8,10]

[1]*Institut de Physique Nucléaire, CNRS-IN2P3, Université Paris-Sud, Université Paris-Saclay, F-91406 Orsay, France*
[2]*Max-Planck-Institut für Kernphysik, Saupfercheckweg 1, D-69117 Heidelberg, Germany*
[3]*CERN European Organization for Nuclear Research, Physics Department, CH-1211 Geneva 23, Switzerland*
[4]*ELI-NP, Horia Hulubei National Institute for R&D in Physics and Nuclear Engineering, 077125 Magurele, Romania*
[5]*School of Physics and Astronomy, The University of Manchester, Manchester, M13 9PL, United Kingdom*
[6]*Instituut voor Kern- en Stralingsfysica, KU Leuven, Celestijnenlaan 200D, 3001 Leuven, Belgium*
[7]*Institut für Kernphysik, Universität zu Köln, Zülpicher Straße 77, D-50937 Köln, Germany*
[8]*Institut für Kernchemie, Johannes Gutenberg-Universität Mainz, D-55128 Mainz, Germany*
[9]*Institut für Kernphysik, Technische Universität Darmstadt, D-64289 Darmstadt, Germany*
[10]*GSI Helmholtzzentrum für Schwerionenforschung GmbH, D-64291 Darmstadt, Germany*

(Received 25 May 2018; published 30 July 2018)

The neutron-deficient cadmium isotopes have been measured by high-resolution laser spectroscopy at CERN-ISOLDE. The electromagnetic moments of ^{101}Cd have been determined for the first time and the quadrupole-moment precision of ^{103}Cd has been vastly improved. The results on the sequence of $5/2^+$ ground states in $^{101-109}$Cd are tentatively discussed in the context of simple structure in complex nuclei as similarities are found with the $11/2^-$ states in the neutron-rich cases. Comparison with shell-model calculations reveals a prominent role of the two holes in the $Z = 50$ core.

DOI: 10.1103/PhysRevC.98.011303

The isotopic chain of cadmium has emerged in recent years as a pivotal case for nuclear-structure studies in the intermediate-mass region, perhaps outweighing tin itself whose closed proton shell is certainly one of the major landmarks in the nuclear landscape. Shell quenching [1], stellar nucleosynthesis [2], and isomerism [3] are some of the topics addressed most recently. With respect to charge radii and electromagnetic moments, simple mass-dependent trends have been observed in the heavier isotopes [4,5] which are yet to be discussed in the tin counterparts. In this text we are exploring the sequence of neutron-deficient isotopes from ^{109}Cd down to ^{101}Cd whose ground states are expected to involve the $d_{5/2}$ shell embedded in the neighboring $g_{7/2}$, $s_{1/2}$, and $d_{3/2}$ orbits, and as such would be unlikely to adopt a simple configuration when compared to the unique-parity $h_{11/2}$ states in the neutron-rich cases. A simplified view on the matter is outlined in the beginning and ultimately examined against large-scale shell-model calculations.

The measurements were carried out with the instrumentation for collinear laser spectroscopy (COLLAPS) at ISOLDE-CERN [6]. The radionuclides of interest were produced by high-energy protons impinging on a molten tin target and ionized using a plasma source. This production arrangement is very efficient [7] for the longer-lived cadmium isotopes discussed here. After 30-kV acceleration and mass selection the ion beams were accumulated in a radio-frequency Paul trap [8] and subsequently released every 100 ms with a temporal width of about 5 μs. The cadmium ions were excited in the transition: $5s\ ^2S_{1/2} \rightarrow 5p\ ^2P_{3/2}$ at 214.5 nm. The corresponding cw laser beam was produced by sequential second-harmonic generation from the output of a titanium-sapphire laser. Chronologically, this was the first instance of frequency quadrupling being utilized for collinear laser spectroscopy. Atomic excitations were detected by the ion-beam fluorescence as a function of the Doppler-shifted laser frequency [6]. The timing structure of the ion beam mentioned above facilitated a background suppression with a factor of the order of 10^4.

Example spectra of the studied isotopes are fitted and presented in Fig. 1. The fit functions utilize free intensities and the empirical line shape from Ref. [9]. Only in ^{107}Cd the relative amplitudes of the fourth and the fifth resonance from the left have been fixed to each other due to a near coincidence of the $F = 3$ and $F = 4$ levels in the $^2P_{3/2}$ multiplet. The hyperfine parameters and electromagnetic moments from this work are presented in Table I and compared to literature values. We have previously published the results on ^{107}Cd and ^{109}Cd since they played a role in the evaluation of the hyperfine anomaly of the $3/2^+$ states in the heavier isotopes [5]. However, their physics case is being addressed in this text.

Previous laser spectroscopy measurements [10] have been Doppler limited. The high-resolution data presented here

*Yordanov@ipno.in2p3.fr

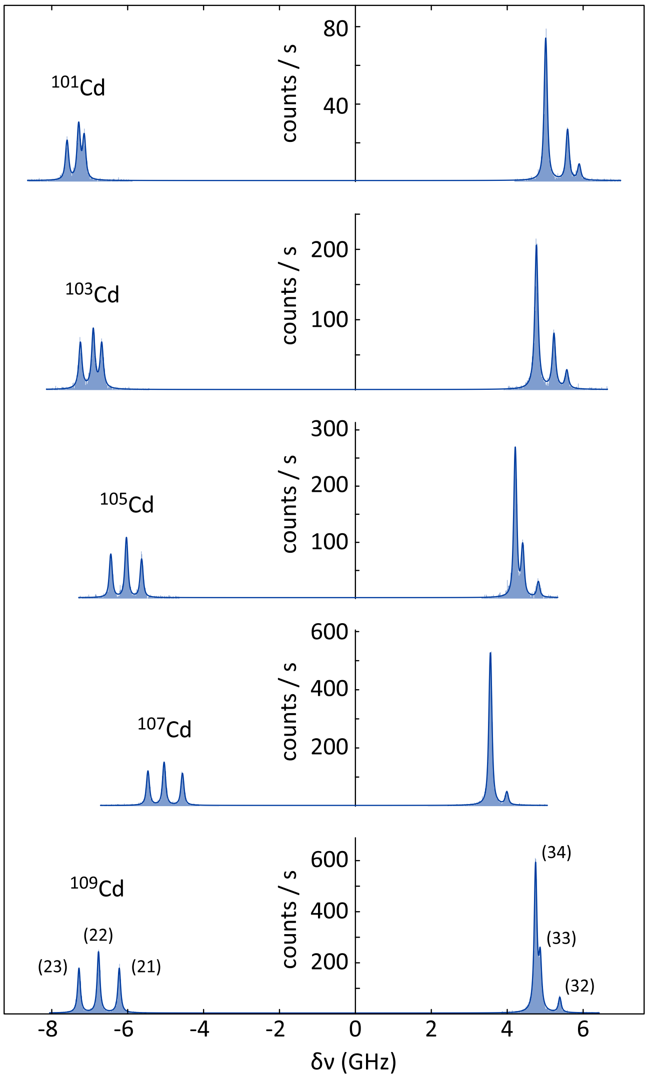

FIG. 1. Example spectra of $^{101-109}$Cd. The hfs level ordering is identical for all cases, as indicated for ^{109}Cd. The frequency scale is relative to the fine-structure splitting.

enable an assessment of the nuclear spin. In all cases the spins are clearly higher than 1/2, otherwise there would have been only three observable transitions instead of six. The relative position of resonances in the spectra of ^{105}Cd, ^{107}Cd, and ^{109}Cd are impossible to describe with any spin other than 5/2 under the condition of a fixed ratio between the $^2S_{1/2}$ and $^2P_{3/2}$ magnetic hyperfine parameters. This result is consistent with the assignments from optical double resonance [11,12], and is further supported by NMR [13]. In both ^{101}Cd and ^{103}Cd, χ^2 analysis under different spin assumptions using the Racah intensities [14] shows a strong minimum at spin 5/2. Spin 3/2 can be ruled out even without evoking the condition of fixed intensities.

The following equations have been used to determine electromagnetic moments from the measured hyperfine parameters:

$$A\frac{I}{\mu} = \text{const}, \tag{1}$$

$$\frac{B}{Q} = \text{const}. \tag{2}$$

The constants above denote the average magnetic field per unit angular momentum and the average electric field gradient induced at the origin by the atomic electrons. For alkali-like multiplets their values are positive, resulting in an identical sign of a given hyperfine parameter and its corresponding nuclear moment. The magnetic moments have been determined from the $^2S_{1/2}$ parameters relative to ^{109}Cd whose magnetic moment [15] is known precisely from NMR frequency ratios [13] and corrected for diamagnetism. All values are negative. Hyperfine anomalies are not deduced because these are extremely small between isotopes of the same spin and similar magnetic moments. The quadrupole moments have been calculated with the electric field gradient 666 (27) MHz/b adopted for the neutron-rich cases [5]. The reduction in absolute value of the quadrupole moments with respect to former measurements [12,16] has been discussed in our previous work [5], and more recently addressed in a multidisciplinary theoretical study [17].

The apparent behavior of the $5/2^+$ electromagnetic moments in $^{101-107}$Cd, as shown in Fig. 2, bears a striking resemblance to the linear trends associated with the $11/2^-$ states in $^{111-129}$Cd [5], as well as other established examples [18–20] involving a unique-parity orbital, either $g_{9/2}$, $h_{11/2}$, or $i_{13/2}$. In the basic case of a j^n configuration the quadrupole moment follows a simple mass dependence [21,22]:

$$\langle j^n|\hat{Q}|j^n\rangle = \frac{2j+1-2n}{2j-1}\langle j|\hat{Q}|j\rangle. \tag{3}$$

TABLE I. Spins, hyperfine parameters, and electromagnetic moments from this work compared with literature values [10–13,15,16]. Statistical uncertainties are shown in parentheses. A second set of parentheses denotes the uncertainty associated with the accuracy of the electric field gradient. The previously published values of ^{107}Cd and ^{109}Cd [5] are given here for completeness.

$Z+N$	I	A (MHz)	A (MHz)	B (MHz)	μ/μ_N	$\mu_{\text{literature}}/\mu_N$	Q (mb)	$Q_{\text{literature}}$ (mb)
101	5/2	−4395.9 (8)	−120.6 (3)	−118 (2)	−0.8983 (2)		−177 (2) (7)	
103	5/2	−4158.6 (7)	−114.3 (2)	−4 (2)	−0.8498 (2)	−0.81 (3)	−7 (3) (0)	−790 (660)
105	5/2	−3617.6 (6)	−99.7 (2)	251 (1)	−0.7393 (2)	−0.7393 (2)	377 (2) (15)	430 (40)
107	5/2	−3009.8 (7)	−82.3 (3)	401 (2)	−0.6151 (2)	−0.6150554 (11)	601 (3) (24)	680 (70)
109	5/2	−4051.0 (7)	−111.4 (2)	403 (1)		−0.8278461 (15)[a]	604 (1) (25)	690 (70)
		$5s\ ^2S_{1/2}$	$5p\ ^2P_{3/2}$					

[a]Magnetic moment of ^{109}Cd [13,15] used for calibration.

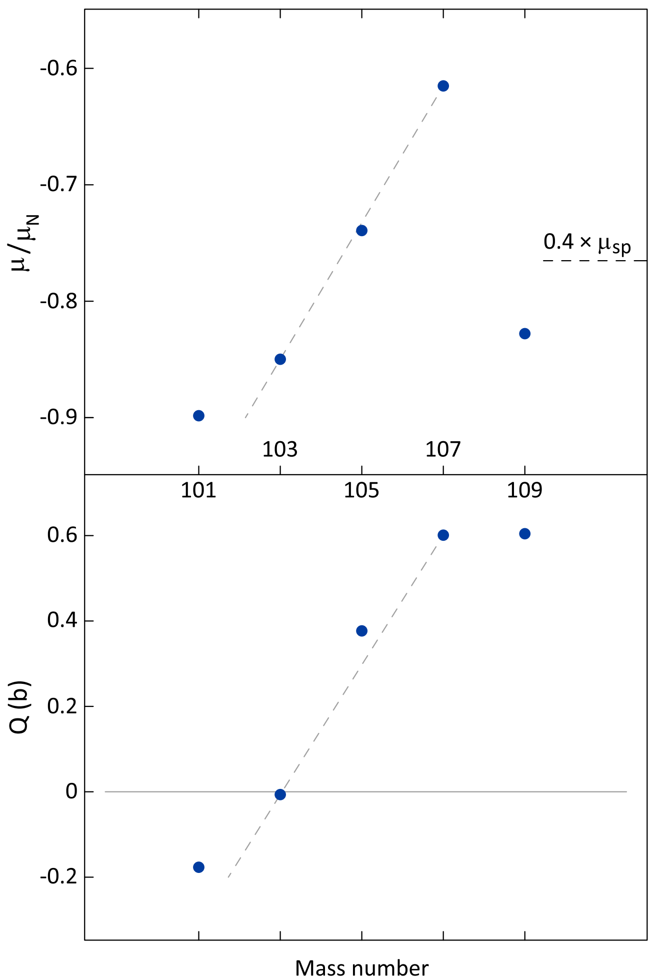

FIG. 2. Ground-state electromagnetic moments of $^{101-109}$Cd from this work. All uncertainties are smaller than the dots. The dashed lines are defined by the values at ^{103}Cd and ^{107}Cd.

The corresponding magnetic moments are expected to remain constant or to exhibit a weak linear deviation induced by core polarization [23,24]. In $^{101-109}$Cd, on the other hand, the odd neutron is not restricted by the parity to a particular orbital. Similar arrangement is at work in the calcium isotopes [25,26] as well as in the $N = 125$, 126 isotones [27], both showing consistency with Eq. (3). Therefore, the evidence for apparent linearity in Fig. 2 is worth investigating. As in our previous work [5] the following substitution can be made:

$$n = 1 + p(A - A_0). \tag{4}$$

The parameters p and A_0 can be easily calculated from the data. First, it would appear that the neutron occupation of $d_{5/2}$ is already at its maximum in ^{107}Cd since the quadrupole moment of ^{109}Cd is identical. Thus, one can formally write $n(107) = 5$. Second, the quadrupole moment of ^{103}Cd from our experiment is practically zero, which according to Eq. (3) occurs for $n = (2j + 1)/2$, therefore $n(103) = 3$. Consequently, one arrives at

$$n = 1 + \frac{A - 99}{2}. \tag{5}$$

Having determined $A_0 = 99$ simply means that there is only one $d_{5/2}$ neutron in ^{99}Cd. And indeed, without particle-hole excitations across $N = 50$ there can be no more. The probability $p = 1/2$ for $d_{5/2}$ occupation corresponds to the number of neutron pairs that can be added to the $d_{5/2}$ shell in addition to an odd neutron, divided by the number of pairs filled between ^{99}Cd and ^{107}Cd. In this interpretation ^{99}Cd would have a quadrupole moment with the opposite sign and identical in magnitude to the 601 mb of ^{107}Cd. In comparison, the size of the single-particle quadrupole moment $-\langle r^2\rangle(2j-1)/(2j+2) = -200$ mb is exactly three times smaller. Here, under the assumption of a uniformly charged spherical nucleus, the mean-square orbital radius is approximated by 5/3 of the mean-square charge radius of ^{111}Cd [28]. The above factor of 3 would indicate that in the proposed simplified picture about 2/3 of the $5/2^+$ quadrupole moments are generated through core polarization. This figure, while similar to the one of the $11/2^-$ states inferred from our previous work [5], is somewhat larger in comparison to a dedicated relativistic mean-field study [29].

A more realistic view on the underlined nuclear structure is obtained by large-scale shell-model calculations carried out with the SR88MHJM Hamiltonian [20,31] using the M-scheme code for massive parallel computation KSHELL [32]. The model space incorporates the orbitals up to the $Z = 50$ and $N = 82$ shell closures outside a hypothetical ^{88}Sr core. Effective spin gyromagnetic ratios at 70% of the free nucleon values and effective charges $e_\nu = e$ and $e_\pi = 1.7e$ were used. The results for the lowest $5/2^+$ states are compared in Fig. 3 to our measurements and the $5/2^+$ isomer in ^{111}Cd [17,30]. For both observables the agreement is fairly good. In the following we offer a simplified analysis of the theoretical output in order to discuss the main features in Fig. 3, and also to assess the relevance of the basic description inferred in the beginning.

One may first consider Fig. 4(a) showing the probability for occurrence of an odd neutron in either and only one of the neutron positive-parity orbitals. For clarity we have presented the occupation of $d_{5/2}$ against the combined contribution from $g_{7/2}$, $d_{3/2}$, and $s_{1/2}$, rather than showing all individually. The latter three would each produce a sizable positive magnetic moment when coupled with a 2^+ proton state. This statement is also valid for $d_{5/2}$, albeit the value is somewhat smaller and strongly dependent on the choice of effective operators. Therefore, the upward trend in the magnetic moments from ^{99}Cd to ^{107}Cd should be understood as a depletion of the single-particle contribution from $d_{5/2}$ in favor of configurations of the type $[(\pi g_{9/2})^{-2}_{2^+} \otimes \nu l_{j^+}]_{5/2^+}$. Conversely, the drop at the ^{109}Cd moment is produced by the opposite effect where the odd-neutron occupation of $d_{5/2}$ is suddenly increased. This occurs almost exclusively at the expense of the $g_{7/2}$ orbital. The emerging picture is different from the one proposed by Byron and co-workers [11] who, on the basis of the configuration-mixing approach of Noya, Arima, and Horie [33], suggested an interplay with the neutron $g_{9/2}$ spin partner. The latter is not present in the SR88MHJM configuration space, and yet the effect is largely reproduced. The value at ^{103}Cd is overestimated in part due to stronger contributions from $s_{1/2}$ and $d_{3/2}$ relative to $g_{7/2}$, as the proton-neutron configurations of the former two generate larger magnetic moments. This

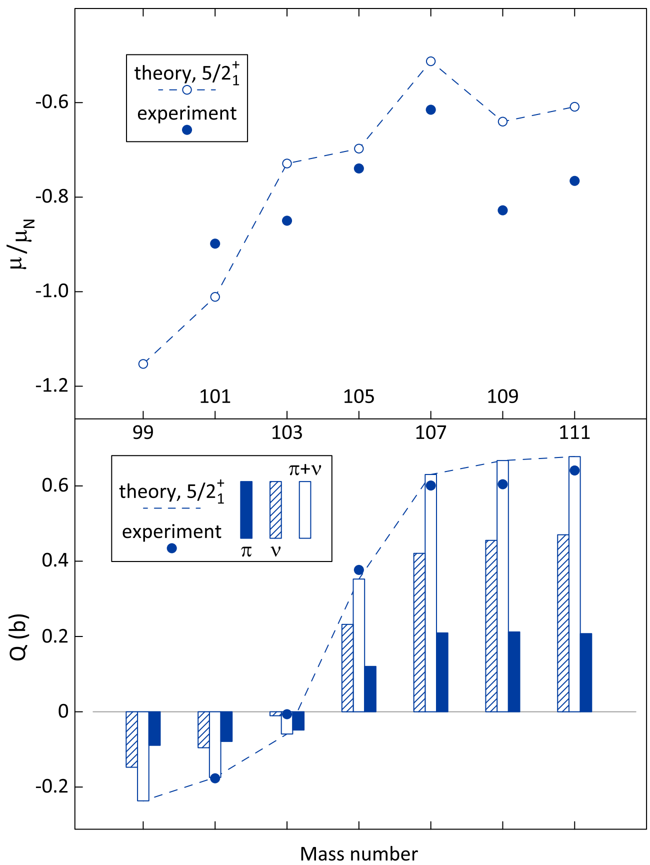

FIG. 3. Electromagnetic moments from theory (opened bars and circles linked by dashed lines) compared to this work and ^{111}Cd [17,30] (filled dots). The experimental uncertainties are smaller than the dots.

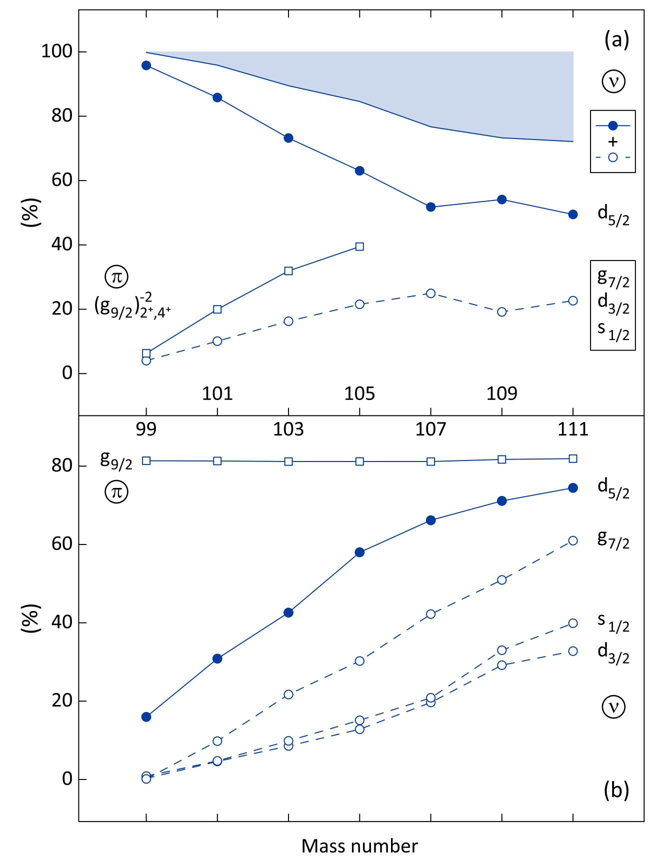

FIG. 4. (a) Odd-neutron occupation of one and only one of the respective orbitals (see text for details). (b) Total population of the respective orbitals in percent. The evolution of the proton $g_{9/2}$ shell is also depicted.

local occurrence contributes to an apparent staggering of the magnetic moments in Fig. 3. Additional calculations with the same interaction using the J-scheme code NuShellX@MSU [34] could be propagated up to ^{105}Cd in order to quantify the amount of $(\pi g_{9/2})^{-2}_{2^+}$ configurations. As shown in Fig. 4(a) the corresponding values rapidly increase toward the middle of the shell, much faster than the summed contribution from the $g_{7/2}$, $d_{3/2}$, and $s_{1/2}$ orbitals. Simultaneously multiparticle configurations of three or a higher number of unpaired nucleons also become abundant, as represented by the shaded area in the figure. An onset of $(\pi g_{9/2})^{-2}_{4^+}$ configurations is also present toward the middle of the shell, rising to about 4% in ^{105}Cd. The negative-parity orbitals $p_{1/2}$ and $h_{11/2}$ are not depicted as their role is limited.

The trend of theoretical quadrupole moments in Fig. 3 appears to deviate from linearity, with the value at ^{103}Cd seemingly being an inflection point. However, there is no prominent feature at this mass in either of the plots in Fig. 4. On the contrary, the occurrence of an odd $d_{5/2}$ neutron in Fig. 4(a) and the total $d_{5/2}$ population in Fig. 4(b) both change regularly between ^{99}Cd and ^{107}Cd. Hence, the role of 2^+ proton configurations requires further investigation. Accordingly, the quadrupole moment is decomposed into a proton- and a neutron-generated part, as shown explicitly in Fig. 3. It is evident that in all cases the proton constituent amounts to about $1/3$ of the total moment, a figure twice smaller than anticipated from the simplistic interpretation above. In the beginning of the shell the quadrupole moment obtains a negative value, followed by a regular increase in accordance with Eq. (3) as a function of the $d_{5/2}$ population. The features on top of this trend should be understood as an interplay between configurations of the type $[(\pi g_{9/2})^{-2}_{2^+} \otimes \nu(l_j)^n_{j^+}]_{5/2^+}$. The corresponding contributions involving $s_{1/2}$ and $d_{3/2}$ neutrons are negative. These cause a prediction at ^{99}Cd below the single-particle value discussed earlier. In the heavier isotopes the quadrupole moment rapidly increases with the filling of the $g_{7/2}$ and $d_{5/2}$ orbitals whose contribution is positive. Toward the end of the studied range the moments appear to incline toward a constant value. This should be attributed in part to a $d_{5/2}$ saturation, and in part to approaching a limit in the amount of non-zero-spin proton couplings which would also change composition to include 4^+ and possibly higher-spin values. On the whole, the observed trend is governed by the $d_{5/2}$ occupation being delayed due to the simultaneous $g_{7/2}$ filling. It is not symmetric to midshell $d_{5/2}$ nor to $Q = 0$, as an increasing proton $g_{9/2}$ contribution is superimposed. For the sake of completeness, we note that the lowest $5/2^+$ states calculated in ^{107}Cd and ^{109}Cd appear at small excitation energies above a $1/2^+$ ground state, respectively, at 59 and 234 keV. In ^{111}Cd the level ordering of the two states is reproduced correctly.

In summary, we have provided accurate ground-state electromagnetic moments for $^{101-105}$Cd. The data are initially discussed in the context of simple structure in complex nuclei [26,35–37]. Large-scale shell-model calculations using the SR88MHJM Hamiltonian firmly establish the significance of the proton $g_{9/2}$ contribution to both electromagnetic moments and the importance of the joined filling, in particular of the close-lying $d_{5/2}$ and $g_{7/2}$ orbitals, for the observed nuclear structure. With regard to the quadrupole moment of ^{99}Cd, −600 mb have been inferred from a simplistic interpretation. The shell-model calculations, on the other hand, support a much weaker value of about −240 mb. A measurement by collinear laser spectroscopy is certainly achievable, and being a closed-shell-plus-one-neutron case of key importance, ^{99}Cd will most certainly receive further attention in the future.

We thank the ISOLDE technical group for their professional assistance. This work has been supported by the Max-Planck Society, the German Federal Ministry for Education and Research under Contract No. 05P12RDCIC, the Belgian IAP Project P7/12, the FWO-Vlaanderen, and the European Union seventh framework through ENSAR under Contract No. 262010. D.L.B. acknowledges support by the Extreme Light Infrastructure Nuclear Physics, a project co-financed by the Romanian Government and the European Union through the European Regional Development Fund – Competitiveness Operational Programme (1/07.07.2016, COP, ID 1334).

[1] I. Dillmann, K.-L. Kratz, A. Wöhr, O. Arndt, B. A. Brown, P. Hoff, M. Hjorth-Jensen, U. Köster, A. N. Ostrowski, B. Pfeiffer, D. Seweryniak, J. Shergur, and W. B. Walters, Phys. Rev. Lett. **91**, 162503 (2003).
[2] D. Atanasov, P. Ascher, K. Blaum, R. B. Cakirli, T. E. Cocolios, S. George, S. Goriely, F. Herfurth, H.-T. Janka, O. Just, M. Kowalska, S. Kreim, D. Kisler, Y. A. Litvinov, D. Lunney, V. Manea, D. Neidherr, M. Rosenbusch, L. Schweikhard, A. Welker, F. Wienholtz, R. N. Wolf, and K. Zuber, Phys. Rev. Lett. **115**, 232501 (2015).
[3] A. Jungclaus *et al.*, Phys. Lett. B **772**, 483 (2017).
[4] D. T. Yordanov, D. L. Balabanski, M. L. Bissell, K. Blaum, I. Budinčević, B. Cheal, K. Flanagan, N. Frömmgen, G. Georgiev, C. Geppert, M. Hammen, M. Kowalska, K. Kreim, A. Krieger, J. Meng, R. Neugart, G. Neyens, W. Nortershauser, M.M. Rajabali, J. Papuga, S. Schmidt, and P. W. Zhao, Phys. Rev. Lett. **116**, 032501 (2016).
[5] D. T. Yordanov, D. L. Balabanski, J. Bieroń, M. L. Bissell, K. Blaum, I. Budinčević, S. Fritzsche, N. Frömmgen, G. Georgiev, C. Geppert, M. Hammen, M. Kowalska, K. Kreim, A. Krieger, R. Neugart, W. Nörtershäuser, J. Papuga, and S. Schmidt, Phys. Rev. Lett. **110**, 192501 (2013).
[6] R. Neugart *et al.*, J. Phys. G **44**, 064002 (2017).
[7] H. J. Kluge, Isolde users' guide, CERN-86-05 (CERN, Geneva, 1986), p. 200, https://cds.cern.ch/collection/ISOLDE%20Reports?ln=en.
[8] E. Mané *et al.*, Eur. Phys. J. A **42**, 503 (2009).
[9] D. T. Yordanov *et al.*, J. Phys. G **44**, 075104 (2017).
[10] F. Buchinger *et al.*, Nucl. Phys. A **462**, 305 (1987).
[11] F. W. Byron, M. N. McDermott, and R. Novick, Phys. Rev. **132**, 1181 (1963).
[12] N. S. Laulainen and M. N. McDermott, Phys. Rev. **177**, 1615 (1969).
[13] P. W. Spence and M. N. McDermott, Phys. Lett. A **42**, 273 (1972).
[14] P. C. Magnante and H. H. Stroke, J. Opt. Soc. Am. **59**, 836 (1969).
[15] P. Raghavan, At. Data Nucl. Data Tables **42**, 189 (1989).
[16] M. N. McDermott and R. Novick, Phys. Rev. **131**, 707 (1963).
[17] H. Haas *et al.*, Europhys. Lett. **117**, 62001 (2017).
[18] G. Neyens, Rep. Prog. Phys. **66**, 633 (2003).
[19] H. Grawe, Lect. Notes Phys. **651**, 33 (2004).
[20] T. Faestermann, M. Górska, and H. Grawe, Prog. Part. Nucl. Phys. **69**, 85 (2013).
[21] H. Horie and A. Arima, Phys. Rev. **99**, 778 (1955).
[22] I. Talmi, *Simple Models of Complex Nuclei* (Harwood Academic, Amsterdam, 1993).
[23] M. Nomura, Phys. Lett. B **40**, 522 (1972).
[24] J. Wouters, N. Severijns, J. Vanhaverbeke, and L. Vanneste, J. Phys. G **17**, 1673 (1991).
[25] R. F. GarciaRuiz, M. L. Bissell, K. Blaum, N. Frömmgen, M. Hammen, J. D. Holt, M. Kowalska, K. Kreim, J. Menéndez, R. Neugart, G. Neyens, W. Nörtershäuser, F. Nowacki, J. Papuga, A. Poves, A. Schwenk, J. Simonis, and D. T. Yordanov, Phys. Rev. C **91**, 041304(R) (2015).
[26] I. Talmi, Phys. Scr. **92**, 083001 (2017).
[27] R. Ferrer, A. Barzakh *et al.*, Nat. Commun. **8**, 14520 (2017).
[28] G. Fricke and K. Heilig, *Nuclear Charge Radii* (Springer, Berlin, 2004).
[29] P. W. Zhao, S. Q. Zhang, and J. Meng, Phys. Rev. C **89**, 011301(R) (2014).
[30] H. Bertschat *et al.*, Z. Phys. **270**, 203 (1974).
[31] O. Kavatsyuk *et al.*, Eur. Phys. J. A **31**, 319 (2007).
[32] N. Shimizu, arXiv:1310.5431.
[33] H. Noya, A. Arima, and H. Horie, Prog. Theor. Phys. Suppl. **8**, 33 (1958).
[34] B. A. Brown and W. Rae, Nucl. Data Sheets **120**, 115 (2014).
[35] A. E. Stuchbery, J. Phys.: Conf. Ser. **366**, 012042 (2012).
[36] J. Wood, Physics **6**, 52 (2013).
[37] P. V. Isacker, Nucl. Phys. News **24**, 23 (2014).